Int. J. Heat Mass Transfer. Vol. 19, pp. 643–649. Pergamon Press 1976. Printed in Great Britain

MAXIMUM BUBBLE DIAMETER, MAXIMUM BUBBLE-GROWTH TIME AND BUBBLE-GROWTH RATE DURING THE SUBCOOLED NUCLEATE FLOW BOILING OF WATER UP TO 17.7 MN/m^2

H. C. ÜNAL

Central Technical Institute TNO, P.O. Box 342, Apeldoorn, The Netherlands

(*Received* 9 *January* 1975)

Abstract—A heat transfer controlled bubble model has yielded three semi-empirical correlations to predict bubble-growth rate, maximum bubble diameter and maximum bubble-growth time for the subcooled nucleate flow boiling of water.

Our data for maximum bubble diameter for 13.9, 15.8 and 17.7 MN/m^2 obtained by the use of a high-speed photographic technique and the data available in the literature were found to fit the correlations. The range of data used is as follows: pressure: 0.1–17.7 MN/m^2; heat flux: 0.47–10.64 MW/m^2; velocity: 0.08–9.15 m/s; subcooling: 3–86 K; maximum bubble diameter: 0.08–1.24 mm; maximum bubble-growth time: 0.175–5 ms.

NOMENCLATURE

- C, a pressure dependent constant [1/K s];
- c, specific heat of heating surface [J/kg K];
- c_p, specific heat of saturated liquid [J/Kg K];
- D, instantaneous bubble diameter [m];
- D_m, maximum bubble diameter [m];
- D_d, diameter of dry area under the bubble [m];
- g, acceleration of gravity [m/s^2];
- h, single phase forced convection heat-transfer coefficient for the heated surface [W/m^2 K];
- h_c, heat-transfer coefficient for the dissipation of heat from the bubble to the surrounding liquid [W/m^2 K];
- k, thermal conductivity [W/m K];
- Nu, Nusselt number;
- P, pressure [N/m^2];
- Pr, Prandtl number;
- Re, Reynolds number;
- q, heat generation per unit area and time at the heating surface [W/m^2];
- q_B, heat flux to bubble from the very thin liquid film under it [W/m^2];
- ΔT_{sat}, initial superheat of the thin liquid layer under the bubble [K];
- ΔT_{sub}, subcooling of the liquid [K];
- t, time [s];
- t_m, maximum bubble-growth time [s];
- v, liquid bulk velocity [m/s].

Greek symbols

- λ, latent heat of evaporation [J/kg];
- μ, viscosity [Ns/m^2];
- ρ, density [kg/m^3];
- σ, surface tension [N/m].

Subscripts

- b, refers to bulk condition;
- l, refers to saturation condition for liquid phase;
- s, refers to heated surface;
- v, refers to saturation condition for vapour.

INTRODUCTION

DETERMINATION of bubble-growth rate, maximum bubble diameter and maximum bubble-growth time for the subcooled nucleate flow boiling of water is of interest for a basic understanding of the phenomenon of subcooled boiling. The maximum bubble diameter and maximum bubble-growth time are closely related to void fraction and heat-transfer rate. So far no predictive equations of broad generality for bubble dynamics during the subcooled nucleate flow boiling of water have appeared in the literature, although experimental data have been presented by Griffith *et al.* [1], Gunther [2], Tolubinsky and Kostanchuk [3], and Treshchev [4]. Therefore, a heat transfer controlled bubble model has been established to derive a correlation for bubble-growth rate, maximum bubble diameter and maximum bubble-growth time.

The model is based on the assumption that a spherical or an ellipsoidal bubble grows on a very thin, partially dried liquid film which is formed between the bubble and the heated surface. During growth, the bubble is assumed to take up heat by the evaporation of the very thin liquid film while it dissipates heat by condensation to the surrounding liquid at its upper half.

Since difficulties were anticipated with a closed-form solution of the multi-dimensional formulation, a lumped formulation of the model has been used.

Experimental investigation of maximum bubble diameters has also been carried out with the aid of a high-speed photography technique at 13.9, 15.8 and 17.7 MN/m^2.

SUBCOOLED FLOW BOILING BUBBLE MODEL

In order to determine bubble-growth rate, maximum bubble diameter and maximum bubble-growth time, a bubble model will be established with the following assumptions:

1. Subcooled nucleate flow boiling is a transition between the forced convection and the fully developed boiling regimes, and is also referred to as "partial

nucleate boiling", "forced-convection surface-boiling", or simply "surface boiling" in the literature.

2. For a given geometry and constant operating conditions (i.e. constant subcooling, velocity, heat flux and pressure) the numerous bubbles produced in subcooled nucleate flow boiling have different maximum diameters and growth times. A statistical approach is therefore required, and these quantities have to be calculated by averaging the quantities for the whole bubble population. The terms "maximum bubble diameter" and "maximum bubble-growth time" used here refer to average values for the whole bubble population.

3. A spherical or an ellipsoidal bubble grows on a very thin partially dried liquid film which is formed between the bubble and the heated surface as schematized in Fig. 1. The formation of a thin liquid film between the bubble and the heating surface has first been postulated by Snyder [5]. Later this postulate has been verified experimentally by Torikai *et al.* [6], Cooper [7], and Cooper and Lloyd [8]. The evidence for the existence of a dry area in the thin liquid film on the heating surface has been presented for atmospheric pressure conditions by Torikai *et al.* [6].

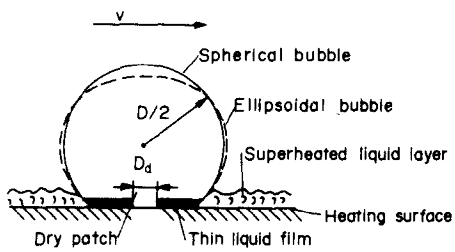

FIG. 1. Schematic bubble description.

4. The instantaneous bubble volume is equal to the volume of a sphere of diameter D.

5. The dry area under the bubble is of circular shape, as experimentally verified by Torikai *et al.* [6].

6. During its growth, the bubble takes up heat by the evaporation of the very thin liquid film over the area $\pi D^2(1-D_d^2/D^2)/4$ in which D_d/D is assumed to be a constant for a given pressure in accordance with the experimental data of Torikai *et al.* [6].

7. Inertia-controlled bubble growth has been neglected since its duration is very short, as experimentally determined by Sernas and Hooper [9].

8. Bubble growth within the superheated liquid layer is neglected since the ratio of the maximum bubble diameter to the thickness of this layer varies between 11 and 25 at atmospheric pressure conditions [10]. This also justifies the assumption that the heat input to the bubble from the superheated layer can be neglected in comparison with the heat from the thin liquid film since the D_d/D is anticipated not to be large.

9. The bubble dissipates heat to the surrounding liquid by condensation at its upper-half surface. In subcooled nucleate flow boiling numerous bubbles cover the heating surface. The bottom half of the bubble therefore will probably not face the cold liquid stream, thus being ineffective in dissipating heat from the bubble. Abdelmessih *et al.* [11] also report that heat dissipation from the bubble occurs at its top.

10. Bubble growth is an isobaric process.

11. In subcooled nucleate flow boiling, there are two types of bubbles in so far as the maximum bubble diameter is concerned. The bubbles formed at high subcoolings do not leave the heated surface, although they attain their maximum diameter. They slide along the heated surface or collapse, as observed visually by Gunther [2]. The bubbles formed at medium or low subcoolings leave the heating surface upon reaching their maximum diameters. The condition for departure from the heated surface can thus be expressed as $\mathrm{d}D/\mathrm{d}t = 0$. The work reported therefore covers the above two types of bubbles.

12. A lumped formulation of the model is considered.

MATHEMATICAL FORMULATION OF THE MODEL AND SOLUTION

Using the above-given assumptions, the energy balance for the bubble yields

$$q_B \frac{\pi D^2}{4}\left(1-\frac{D_d^2}{D^2}\right) = h_c \Delta T_{\mathrm{sub}} \frac{\pi D^2}{2} + \frac{\pi}{6}\rho_v \lambda \frac{\mathrm{d}D^3}{\mathrm{d}t} \quad (1)$$

with the initial condition

$$t = 0 \qquad D = 0.$$

q_B in equation (1), the heat flux to the bubble from the very thin liquid film under it, has been given by Sernas and Hooper [9] as follows:

$$q_B = \frac{\Delta T_{\mathrm{sat}} \gamma k_l}{(\pi \alpha_l t)^{\frac{1}{2}}} \quad (2)$$

where

$$\alpha_l = \frac{k_l}{\rho_l c_{pl}}$$

$$\gamma = \left(\frac{k_s \rho_s c_s}{k_l \rho_l c_{pl}}\right)^{\frac{1}{2}}.$$

ΔT_{sat} in equation (2), the initial superheat of the very thin liquid layer under the bubble has been evaluated with a correlation given in [12], which is in fact a modification of the Rohsenow's superposition method to determine subcooled nucleate flow boiling heat transfer [13]:

$$\Delta T_{\mathrm{sat}} = \left(\frac{q - h\Delta T_{\mathrm{sub}}}{C_1}\right)^{\frac{1}{3}} \quad (3)$$

where

$$C_1 = \frac{\lambda \mu_l \left(\frac{c_p}{0.013 \lambda Pr^{1.7}}\right)_l^3}{[\sigma/(\rho_l-\rho_v)g]^{\frac{1}{2}}}$$

and h follows from the well-known relation $Nu_b Re_b^{-0.8} Pr_b^{-\frac{1}{3}} = \text{Constant}$, where the constant equals 0.0366 for flat plates and 0.023 for circular tubes.

h_c in equation (1), the heat-transfer coefficient for condensation at the surface of the bubble, has been derived in [10] with a method analogous to that given by Levenspiel [14], and is equal to

$$h_c = \frac{C\Phi\lambda D}{2(1/\rho_v - 1/\rho_l)} \tag{4}$$

where

$$\Phi = \left(\frac{v}{v_0}\right)^{0.47} \quad \text{for} \quad v > 0.61\,\text{m/s}$$

$$\Phi = 1 \quad \text{for} \quad v \leqslant 0.61\,\text{m/s}$$

$$v_0 = 0.61\,\text{m/s}$$

and C is a pressure-dependent constant, equal to 61 $(\text{K s})^{-1}$ at 0.17 MN/m^2 [10]. For pressures higher and lower respectively than 0.17 MN/m^2 the determination of C will be given later.

Substituting equations (2) and (4) in equation (1) and differentiating the second term of its R.H.S. yields

$$\frac{\mathrm{d}D}{\mathrm{d}t} = a\alpha t^{-1/2} - C\Phi bD \tag{5}$$

where

$$a = \frac{(q - h\,\Delta T_{\text{sub}})^{1/3} k_l \gamma}{2C_1^{1/3}\rho_v \lambda(\pi\alpha_1)^{1/2}} \tag{5.1}$$

$$b = \frac{\Delta T_{\text{sub}}}{2(1-\rho_v/\rho_l)} \tag{5.2}$$

$$\alpha = (1 - D_d^2/D^2). \tag{5.3}$$

Solution of equation (5), which is presented in Appendix 1, gives bubble diameter as a function of time:

$$D(t) = \frac{2a\alpha t^{1/2}[1 + \frac{1}{3}bC\Phi t]}{[1 + C\Phi bt]}. \tag{6}$$

When the bubble reaches its maximum (or departure) diameter, equations (5) and (6) give

$$t_m^{1/2} = \frac{a\alpha}{C\Phi bD_m} \tag{7}$$

$$D_m = \frac{2a\alpha t_m^{1/2}[1 + \frac{1}{3}bC\Phi t_m]}{[1 + C\Phi bt_m]} \tag{8}$$

since

$$\frac{\mathrm{d}D}{\mathrm{d}t} = 0 \quad \text{and} \quad D(t_m) = D_m \quad \text{when} \quad t = t_m.$$

The maximum bubble-departure diameter and maximum bubble-growth time can be then found from the solution of the above two equations

$$D_m = 1.21\frac{a\alpha}{(bC\Phi)^{1/2}} \tag{9}$$

$$t_m = \frac{1}{1.46bC\Phi}. \tag{10}$$

To be able to calculate $D(t)$, D_m and t_m with the aid of equations (6), (9) and (10), α and C have to be known. First, $\alpha/C^{1/2}$ will be determined. Equation (9) can be written in a different and open form:

$$\frac{D_m(\Phi\Delta T_{\text{sub}})^{1/2}}{(q - h\,\Delta T_{\text{sub}})^{1/3}(k_s\rho_s c_s)^{1/2}} = \frac{0.605\alpha[2(1-\rho_v/\rho_l)]^{1/2}k_l}{C^{1/2}\rho_v\lambda C_1^{1/3}(\pi\alpha_1)^{1/2}(k_l\rho_l c_{pl})^{1/2}} \tag{11}$$

The R.H.S. of equation (11) contains only pressure-dependent variables; it is therefore a constant for a given pressure. In order to verify this, the L.H.S. of it will be used since α and C on the R.H.S. are not known. For a wide pressure range, the L.H.S. of equation (11) can be determined using the experimental data of Griffith *et al.* [1], Gunther[2], Tolubinsky and Kostanchuk [3], and Treshchev [4], which is given in Appendix 2, and our data given in Table 1, since the L.H.S. of this equation contains only measured quantities (D_m, v, ΔT_{sub}, q) or predictable quantities (h, k_s, ρ_s, c_s). To this end the L.H.S. of equation (11) has been plotted vs pressure as shown in Fig. 2. From this figure it can be concluded that as a first approximation the L.H.S. or R.H.S. of equation (11) is a constant for a given pressure within reasonable accuracy limits. Furthermore, Fig. 2 shows that the L.H.S. or R.H.S. of equation (11) is a constant for the whole pressure range between 1 and 17.7 MN/m^2.

Having verified that $\alpha/C^{1/2}$ is a pressure-dependent constant, its numerical value can be found by plotting vs pressure the value of $[D_m(b\Phi)^{1/2}/1.21a]$ [see equation (9)]—which can be calculated by using the experimental data of the aforesaid investigators given in Appendix 2, and our data given in Table 1—as shown in Fig. 3:

$$\frac{\alpha}{C^{1/2}} = 2.10^{-5}P^{0.709}. \tag{12}$$

By substituting equation (12) into equation (9), the maximum bubble diameter becomes

$$D_m = \frac{2.42\,10^{-5}P^{0.709}a}{(b\Phi)^{1/2}}. \tag{13}$$

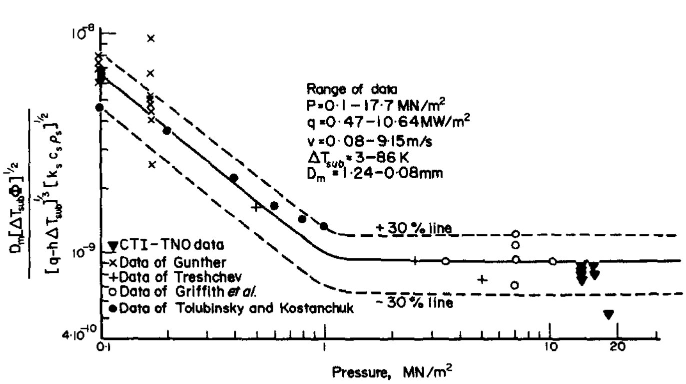

FIG. 2. Verification of equation (11).

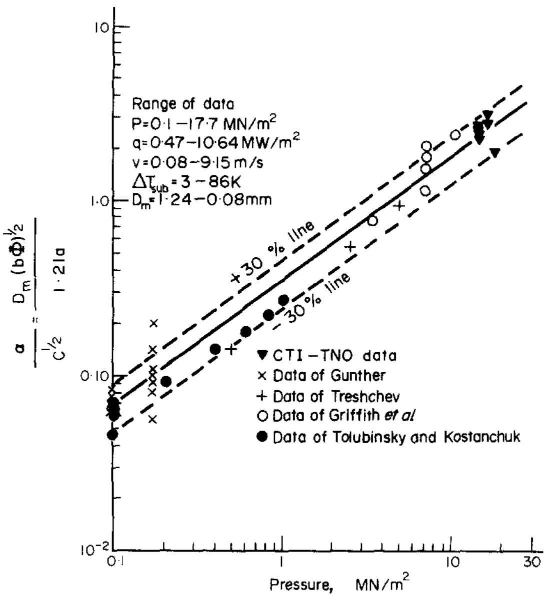

FIG. 3. Maximum bubble diameter correlation.

The experimental range of the above equation is:

$P = 0.1\text{–}17.7\,\mathrm{MN/m^2}$
$q = 0.47\text{–}10.64\,\mathrm{MW/m^2}$
$v = 0.08\text{–}9.15\,\mathrm{m/s}$
$\Delta T_{sub} = 3\text{–}86\,\mathrm{K}$
$D_m = 0.08\text{–}1.24\,\mathrm{mm}$.

Although $(\alpha/C^{\frac{1}{2}})$ has been determined, α and C cannot be found yet, since no other relation between them can be established. Therefore, to predict α and C, the following procedure has been adopted. Figure 2 shows that there is an essential variation in the mechanism of bubble growth at about $1\,\mathrm{MN/m^2}$. For this pressure, inserting into equation (10) the experimental data of Tolubinsky and Kostanchuk given in Appendix 2 (i.e. values of t_m, D_m, ΔT_{sub}, v and q), C is found to be $13.7\ (\mathrm{K\,s})^{-1}$. With the aid of this C-value and equations (9) and (5.3), $D_d\,(t_m)$, the diameter of the dry area under the bubble, is found to be $D_d\,(t_m) = 0.04\,D_m$.

The average value of $D_d(t_m)$ can also be calculated for $0.17\,\mathrm{MN/m^2}$ as $D_d(t_m) = 0.53 D_m$ by using equations (9) and (5.3) and the data of Gunther for eight bubbles given in the Appendix 2, since C is known for this pressure, as stated before. Comparison of these two $D_d(t_m)$ values shows that the dry area under the bubble disappears at about $1\,\mathrm{MN/m^2}$. Therefore:

$$\alpha = (1 - D_d^2/D^2) \cong 1 \qquad 1 < P[\mathrm{MN/m^2}] \leqslant 17.7. \quad (14)$$

For the above-given pressure range, C can then be calculated from equation (12) by using $\alpha = 1$, as follows:

$$C = 0.25\cdot 10^{+10} P^{-1.418} \quad \text{for} \quad 1 < P[\mathrm{MN/m^2}] \leqslant 17.7. \quad (15)$$

Up to $1\,\mathrm{MN/m^2}$, due to lack of experimental data, C may be determined by linear interpolation and extrapolation using the values of C found for 0.17 and $1\,\mathrm{MN/m^2}$, i.e.

$$C = 65 - 5.69\cdot 10^{-5}(P - 10^5) \quad \text{for} \quad 0.1 \leqslant P[\mathrm{MN/m^2}] \leqslant 1. \quad (16)$$

For the above-given pressure range, α can be found from equation (12) by substituting equation (16) into it as follows

$$\alpha = 2\cdot 10^{-5} P^{0.709}[65 - 5.69\cdot 10^{-5}(P - 10^5)]^{\frac{1}{2}} \quad \text{for} \quad 0.1 \leqslant P[\mathrm{MN/m^2}] \leqslant 1. \quad (17)$$

The above-given C and α values have to be substituted into equations (5), (6) and (10) to determine bubble-growth rate, instantaneous bubble diameter and maximum bubble-growth time.

First, the experimental data of Gunther [2], and Tolubinsky and Kostanchuk [3] for maximum bubble-growth times given in the Appendix 2 have been compared with those predicted by equation (10), as shown in Fig. 4. Equation (10) predicts well the

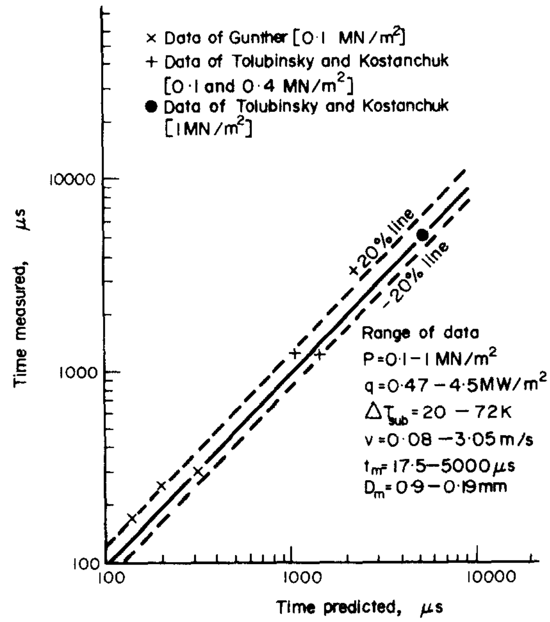

FIG. 4. Comparison of experimental and predicted maximum-bubble growth times.

maximum bubble-growth time within 20%. The experimental range of this correlation is:

$P = 0.1\text{–}1\,\mathrm{MN/m^2}$
$q = 0.47\text{–}4.5\,\mathrm{MW/m^2}$
$\Delta T_{sub} = 20\text{–}72\,\mathrm{K}$
$v = 0.08\text{–}3.05\,\mathrm{m/s}$
$t_m = 0.175\text{–}5\,\mathrm{ms}$
$D_m = 0.19\text{–}0.9\,\mathrm{mm}$.

As a last step, the instantaneous bubble diameter predicted by equation (6) has been compared with the data of Gunther [2], as shown in Fig. 5. It appears that the predicted diameter of the average bubble fits the data quite well. The average maximum diameter of the bubble population, D_m in Fig. 5, has been indicated by Gunther.

EXPERIMENTAL DATA

Maximum bubble diameters have also been determined experimentally for the subcooled nucleate flow boiling of water at high pressures by a high-speed

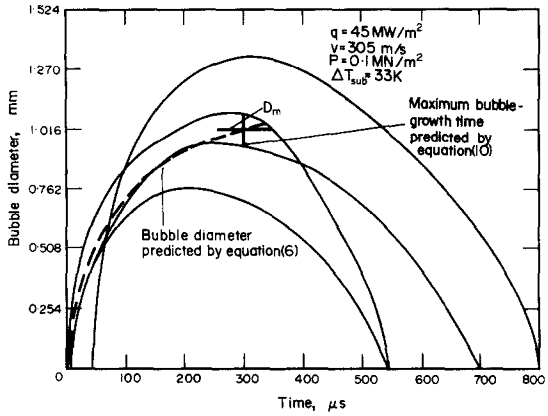

FIG. 5. Comparison of experimental and predicted bubble diameters.

photographic technique. The results are given in Table I. The experimental set-up is described elsewhere in detail by De Munk [15]. The photographical test section was an adiabatic cylindrical sapphire of 8 mm I.D. and 20 mm height, mounted just at the end of a 10 m long sodium heated steam generator pipe.

The films of the bubbles have been taken through the sapphire test section with a framing camera (Dynafax, model 350) at a frequency of 5000 frames per second. The developed films have been enlarged up to 18 times, and the diameters of bubbles appearing on the films have been measured. The bubble population per picture varied between 65 and 450. The distribution of the maximum bubble diameter approximated a normal distribution, thus making the averaging procedures easier.

Table 1. Data for maximum bubble diameter

P (MN/m^2)	ΔT_{sub} (K)	v (m/s)	q (MW/m^2)	D_m (mm)
13.9	3.7	3.27	0.38	0.15
13.9	4.3	3.27	0.39	0.14
13.9	3.7	3.27	0.42	0.18
13.9	5.9	3.27	0.39	0.11
15.8	4.1	3.57	0.45	0.15
15.8	4.1	3.57	0.45	0.13
17.7	3	3.75	0.55	0.13

Acknowledgement—This study has been performed under the auspices of the Project Group for Nuclear Energy TNO. The author wishes to express his gratitude to Mr. M. L. G. van Gasselt for his encouragement during the preparation of this work.

REFERENCES

1. P. Griffith, J. A. Clark and W. M. Rohsenow, Void volumes in subcooled boiling systems, ASME Paper No. 58-HT-19 (1958).
2. F. C. Gunther, Photographic study of surface-boiling heat transfer to water with forced convection, *Trans. Am. Soc. Mech. Engrs* **73**, 115–123 (1951).
3. V. I. Tolubinsky and D. M. Kostanchuk, Vapour bubbles growth rate and heat transfer intensity at subcooled water boiling, *Heat Transfer 1970*, Preprints of papers presented at the Fourth International Heat Transfer Conference, Paris-Versailles 1970, Vol. 5, Paper No. B2.8.
4. G. G. Treshchev, The number of vapor-formation centers in surface boiling, in *Convective Heat Transfer in Two-Phase and One-Phase Flows*, edited by V. M. Borishanskii and I. I. Paleev, pp. 97–105. Israel Program for Scientific Translations, Jerusalem (1969).
5. N. W. Snyder and T. T. Robin, Mass-transfer model in subcooled nucleate boiling, *J. Heat Transfer* **91**, 404–412 (1969).
6. K. Torikai, M. Hori, M. Akiyama, T. Kobori and H. Adachi, Boiling heat transfer and burnout mechanism in boiling-water cooled reactor. Third United Nations International Conference on the Peaceful Uses of Atomic Energy, Paper No. 28/P/580 (1964).
7. M. G. Cooper, The microlayer and bubble growth in nucleate pool boiling, *Int. J. Heat Mass Transfer* **12**, 915–934 (1969).
8. M. G. Cooper and A. J. P. Lloyd, Transient local heat flux in nucleate boiling, *Proceedings of Third International Heat Transfer Conference, Chicago, Illinois, 7–12 August* 1966, Vol. III, pp. 193–203. A.I.Ch.E., New York (1966).
9. V. Sernas and F. C. Hooper, The initial vapor bubble growth on a heated wall during nucleate boiling, *Int. J. Heat Mass Transfer* **12**, 1627–1639 (1969).
10. H. C. Ünal, Bubble-departure diameter, bubble-growth time and bubble-growth rate during the subcooled nucleate flow boiling of water up to 177 bar, Ref. No. 73-02829, Central Technical Institute TNO, P.O. Box 342, Apeldoorn, The Netherlands (1973).
11. A. H. Abdelmessih, F. C. Hooper and S. Nangia, Flow effects on bubble growth and collapse in surface boiling, *Int. J. Heat Mass Transfer* **15**, 115–125 (1972).
12. H. C. Ünal, Heat Transfer to a subcooled boiling liquid and initial point of net vapour generation in forced convection systems, Ref. No. 71-03605, Central Technical Institute TNO, P.O. Box 342, Apeldoorn, The Netherlands (1971).
13. W. M. Rohsenow, Heat transfer with evaporation, University of Michigan Press (1953).
14. O. Levenspiel, Collapse of steam bubbles in water, *Ind. Engng Chem.* **51**, 787–790 (1959).
15. P. J. de Munk, Two-phase flow experiments in a 10 m long sodium heated steam generator test section, *Proceedings of International Meeting on Reactor Heat Transfer*, Karlsruhe, October 9–11, pp. 504–518 (1973).

APPENDIX 1

Solution of Equation (5)

Equation (5) is a linear first-order differential equation, and its solution may be written straightforwardly:

$$D = \mathrm{e}^{-C\Phi bt}\left[\int a\alpha t^{-\frac{1}{2}}\,\mathrm{e}^{C\Phi bt}\,\mathrm{d}t + C_4\right] \tag{A.1}$$

$\mathrm{e}^{C\Phi bt}$ and $\mathrm{e}^{C\Phi bt}$ may be replaced by their identities given in series:

$$D = \frac{a\alpha\int\left[t^{-\frac{1}{2}}(1 + C\Phi bt + C^2\Phi^2b^2t^2/2! + C^3\Phi^3b^3t^3/3! + \cdots)\right]\mathrm{d}t + C_4}{(1 + C\Phi bt + C^2\Phi^2b^2t^2/2! + \cdots)}. \tag{A.2}$$

After integration of the nominator, equation (A.2) becomes:

$$D = \frac{2a\alpha t^{\frac{1}{2}}(1 + 1/3C\Phi bt + 1/10C^2\Phi^2b^2t^2 + \cdots) + C_4}{(1 + C\Phi bt + C^2\Phi^2b^2t^2/2! + \cdots)}. \tag{A.3}$$

By the use of the initial condition, i.e. $D = 0$ for $t = 0$, C_4, the integration constant in equation (A.3) is found to be equal to zero. Experimental data of Gunther [2], and Tolubinsky and of Kostanchuk [3] show that $C\Phi bt_m < 1$ at 0.1 MN/m^2. (In the calculation of $C\Phi bt_m$, the value of C determined for 0.17 MN/m^2 is used, since C is a function of the fluid properties alone, and its value at 0.1 MN/m^2 will therefore not differ much from that at 0.17 MN/m^2.) Thus, when the high-order terms in equation (A.3) are neglected, it becomes:

$$D(t) = \frac{2a\alpha t^{\frac{1}{2}}[1 + 1/3C\Phi bt]}{1 + C\Phi bt}. \tag{A.4}$$

APPENDIX 2

Experimental Data for Maximum Bubble Diameter and Maximum Bubble Growth Time from Various Investigators

Bubble number	Pressure (MN/m^2)	Maximum bubble diameter (mm)	Sub-cooling (K)	Velocity (m/s)	Maximum bubble growth time (μs)	Heat flux (MW/m^2)	Type and dimension of the heating surface (mm)	Investigator
1	0.1	1.24	5	0.20	—	0.47	stainless steel plate 55 × 2.5†	Tolubinsky and Kostanchuk [3]
2	0.1	0.9	20	0.20	1200	0.47	as above	as above
3	0.1	0.56	40	0.20	—	0.47	as above	as above
4	0.1	0.47	60	0.20	—	0.47	as above	as above
5	0.1	0.76	72	3.05	175	4.50	stainless steel plate 63.5 × 4.8†	Gunther [2]
6	0.1	0.88	50	3.05	250	4.50	as above	as above
7	0.1	1.02	33	3.05	300	4.50	as above	as above
8	0.1	0.55	85	3.05	—	4.50	as above	as above
9	0.17	0.62	83	1.50	200*	6.14	as above	as above
10	0.17	0.50	83	3.05	125*	6.14	as above	as above
11	0.17	0.36	83	6.10	83*	6.14	as above	as above
12	0.17	0.58	86	3.05	—	2.30	as above	as above
13	0.17	0.58	86	3.05	—	4.50	as above	as above
14	0.17	0.51	86	3.05	—	6.14	as above	as above
15	0.17	0.44	86	3.05	—	8.06	as above	as above
16	0.17	0.32	86	3.05	—	10.64	as above	as above
17	0.2	0.5	20	0.08	—	0.47	same as given for bubble number 1	same as given for bubble number 1
18	0.4	0.3	20	0.08	1200	0.47	as above	as above
19	0.5	0.26	30	1.9	—	1.40	nickel plate 32 × 5.1‡	Treshchev [4]
20	0.6	0.23	20	0.08	—	0.47	same as given for bubble number 1	same as given for bubble number 1
21	0.8	0.20	20	0.08	—	0.47	as above	as above
22	1.0	0.19	20	0.08	5000	0.47	as above	as above
23	2.5	0.14	54	1.9	—	2.03	same as given for bubble number 19	same as given for bubble number 19
24	3.45	0.095	51	6.1	—	6.38	stainless steel plate 12.7 × 9.5†	Griffith *et al.* [1]
25	5.0	0.12	62	1.9	—	2.90	same as given for bubble number 19	same as given for bubble number 19
26	6.9	0.106	39	6.1	—	3.95	same as given for bubble number 24	same as given for bubble number 24
27	6.9	0.146	11	6.1	—	3.25	as above	as above
28	6.9	0.082	53	9.15	—	7.01	as above	as above
29	6.9	0.088	54	9.15	—	5.75	as above	as above
30	10.3	0.081	80	6.1	—	8.53	as above	as above

*The value given is not the bubble-growth time but the bubble-life time.
†In order to evaluate the physical properties of stainless steel, stainless steel, type 304 (austenitic) 18-8S, is considered.
‡In order to evaluate the physical properties of nickel, nickel of 99.97% purity is considered.

LE DIAMETRE MAXIMAL D'UNE BULLE, LA DUREE MAXIMALE DE CROISSANCE D'UNE BULLE ET LA VITESSE DE CROISSANCE D'UNE BULLE LORS D'UNE EBULLITION EN ECOULEMENT NUCLEE SOUS-REFROIDIE DE L'EAU POUR DES PRESSIONS JUSQU'A 17,7 MN/m²

Résumé—Un modèle mathématique d'une bulle contrôlé par le transport de chaleur a produit trois corrélations semi-empiriques pour la prévision de la vitesse de croissance d'une bulle, du diamètre maximal d'une bulle et de la durée maximale de croissance d'une bulle pour l'ébullition en écoulement nucleé sousrefroidie de l'eau.

Nos résultats pour le diamètre maximal d'une bulle pour 13,9, 15,8 et 17,7 MN/m^2, obtenus au moyen de photographie ultra-rapide et les données qui existent dans la littérature ont été trouvés de convenir aux corrélations.

La région de données corrélées est la suivante: pression: 0,1–17,7 MN/m^2; flux de chaleur 0,47–10,64 MW/m^2; vitesse: 0,08–9,15 m/s; sous-refroidissement: 3–86 K; diamètre maximal d'une bulle: 0,08–1,24 mm; durée maximale de croissance d'une bulle: 0,175–5 ms.

MAXIMALER BLASENDURCHMESSER, MAXIMALE BLASENWACHSTUMSDAUER UND BLASENWACHSTUMSGESCHWINDIGKEIT WÄHREND DER UNTERKÜHLTEN SIEDESTRÖMUNG VON WASSER BEI DRÜCKEN BIS ZU 17,7 MN/m²

Zusammenfassung—Ein mathematisches Modell, das auf dem Wärmetransportmechanismus basiert, ergibt drei semi-empirische Korrelationen, welche es ermöglichen, die Blasenwachstumsgeschwindigkeit, den maximalen Blasendurchmesser und die maximale Blasenwachstumsdauer für die unterkühlte Siedeströmung von Wasser vorauszusagen.

Es hat sich herausgestellt, dasz unsere Ergebnisse für den maximalen Blasendurchmesser für 13,9, 15,8 und 17,7 MN/m^2, welche mittels Hochgeschwindigkeitsphotographie ermittelt wurden und die aus der Literatur erhaltenen Daten sich den Korrelationen gut anpassen.

Die Daten liegen im folgenden Bereich: Druck: 0,1–17,7 MN/m^2; Wärmestromdichte: 0,47–10,64 MW/m^2; Geschwindigkeit: 0,08–9,15 m/s; Unterkühlung: 3–86 K; maximaler Blasendurchmesser: 0,08–1,24 mm; maximale Blasenwachstumsdauer: 0,175–5 ms.

МАКСИМАЛЬНЫЙ ДИАМЕТР, МАКСИМАЛЬНОЕ ВРЕМЯ И СКОРОСТЬ РОСТА ПУЗЫРЬКОВ ПРИ ПУЗЫРЬКОВОМ КИПЕНИИ НЕДОГРЕТОЙ ВОДЫ В ПОТОКЕ ПРИ ВЕЛИЧИНЕ ТЕПЛОВОГО ПОТОКА ДО 17,7 Мн/м²

Аннотация — С помощью модели роста пузырьков получено три полуэмпирических соотношения для расчета скорости роста, максимального диаметра и максимального времени роста пузырьков при пузырьковом кипении недогретой воды в потоке. Найдено, что полученными соотношениями описываются наши данные по максимальному диаметру пузырьков при значениях теплового потока, равных 13,9; 15,8 и 17,7 Мн/м², полученные с помощью метода скоростной съемки, и данные, имеющиеся в литературе. Параметры изменялись в следующих диапазонах: давление — от 0,1 до 17,7 Мн/м², тепловой поток — 0,47–10,64 Мвт/м², скорость — 0,08–9,15 м/сек, недогрев — 3–96 К, максимальный диаметр пузырьков — 0,08–1,24 мм, максимальное время роста пузырьков — 0,175–5 мсек.